Positronium formation for positron scattering from metastable hydrogen*

Lin Lin(林蔺), Hong-Nian Wang(汪宏年), and Li-Guang Jiao(焦利光)†

College of Physics, Jilin University, Changchun 130012, *China*

(Received 16 November 2016; revised manuscript received 3 January 2016; published online 13 February 2017)

Positronium (Ps) formation for positron impact on metastable hydrogen in 2s state has been studied by using the two-channel, two-center eikonal final state-continuum initial distorted wave (EFS-CDW) method. The differential, integrated, and total cross sections for Ps formation in different states have been calculated from each channel opening thresholds to high energy region. The results are compared with other theoretical calculations available in the literature. For Ps formation in s-state at intermediate and high energies, our results are in good agreement with the prediction of distorted wave theory. Those formed in p-states and the total Ps formation cross sections are reported for the first time. It is shown that the total Ps formation cross sections for positron scattering from H(2s) state are significantly larger at relatively low energies, while smaller at high energies, compared with those obtained from hydrogen in ground state.

Keywords: positronium formation, metastable hydrogen, continuum distorted wave method

PACS: 34.80.Lx, 34.80.Uv, 36.10.Dr **DOI:** 10.1088/1674-1056/26/3/033401

1. Introduction

Positronium (Ps) formation is one of the most fundamental charge rearrangement processes in positron scattering from atoms, molecules, and solid materials, and it plays important roles in many aspects of researches and applications.[1–4] For Ps formation from the ground state of atoms by positron impact, it has been extensively investigated by various theoretical methods as well as experimental measurements over the past few decades.[5,6] However, for target atoms in excited metastable state, it has rarely been reported in the literature. It is the same situation even for the most simplest target, hydrogen atom. In recent years, the excitation and ionization processes of metastable hydrogen in 2s state by positron impact and many other scattering processes by electron, proton, and anti-proton impact have attracted considerable interests and abundant phenomena were found.[7–10] The Ps formation process of the metastable hydrogen has not been extensively investigated so far.

For positron scattering from the 2s metastable state of H, Ps formation channel is open starting from zero collision energy (−3.4 eV) which is a great challenge for theoretical considerations. The pioneering work on the Ps formation of positron-H(2s) scattering was performed by Fojón *et al.*[11,12] using the Coulomb Born approximation (CBA). Only the formation of Ps in ground state was investigated and it has been shown that the integrated cross sections for H(2s) is significantly larger than those for H(1s) at low energies. However, their results increase significantly as the incident energy approaches to the threshold from higher energies. Recently, Ghoshal and Mandal[13] successfully developed a distorted-wave theory (DWT) in the momentum space and applied it together with the first Born approximation (FBA) to study Ps formation in an arbitrary s-state from an arbitrary s-state of hydrogen atom by positron impact. Both differential and integrated cross sections were reported for intermediate- and high-energy regions. The interests of Ps formation for metastable hydrogen atoms in weakly coupled and dense quantum plasmas were discussed by Nayek and Ghoshal,[14,15] and it is realized that the accuracy of the cross section in plasma environment depends on its value in pure Coulomb situation. Another interesting metastable target that is worth to be mentioned here is the helium atom in $1s2s^3S$ state for which the Ps formation threshold is also negative (−2.06 eV). A four-body version of the continuum distorted wave-final state (CDWFS) model by Hanssen *et al.*[16] and the two-center convergent close-coupling (CCC) method by Utamuratov *et al.*[17] have been applied to such target. It is generally concluded by these authors that the cross sections for positron scattering from this metastable state of helium are significantly larger than those obtained for the ground state, a similar trend as predicted for hydrogen atom. To the best of our knowledge, no direct measurement of the Ps formation for positron impact on metastable state of either H or He is reported up to now.

In our previous work,[18–20] we have developed the two-center, two-channel eikonal final state continuum initial distorted wave (EFS-CDW) method proposed originally by Macri *et al.*[21,22] to study the Ps formation in arbitrary final states for neutral hydrogen atom and hydrogen-like ions by positron impact from low to high energies. All our previous work were done for targets in their ground states and the calculated

*Project supported by the National Natural Science Foundation of China (Grant No. 11504128).

†Corresponding author. E-mail: lgjiao@jlu.edu.cn

© 2017 Chinese Physical Society and IOP Publishing Ltd

results compare nicely with experimental measurements and other state-of-art theoretical methods available in the literature. Great advantages of this method are, e.g., it can be used to calculate Ps formation into arbitrary final states for both neutral and ionized targets and it is more accurate than other perturbation-based theoretical methods at low energies while keeping its simplicity and straightforwardness. In this work, we apply the EFS-CDW method to study the Ps formation process from the metastable hydrogen in 2s state by positron impact. Differential, integrated, and total Ps formation cross sections will be calculated and compared with other theoretical calculations in detail.

Our paper is organized as follows. In Section 2, we briefly outline the EFS-CDW method with special emphasis on its relationship with the Born expansion series. The differential and integrated cross sections for Ps($n = 1$–4) in s- and p-state and the total Ps formation cross sections are shown and compared with other theoretical predictions in Section 3. Section 4 gives a summary of the present work. Atomic units (a.u.) are used throughout the work unless otherwise stated.

2. Theoretical details

A detailed description of the EFS-CDW model to study the Ps formation in arbitrary states by positron scattering from atoms or ions can be found in our previous work.[18–20] Here, we briefly review the essential features of the method. Unlike the process in other distorted-wave formalisms where a distortion potential is constructed initially and from which the distorted wave can be obtained, we firstly define the initial and final states of the scattering system by continuum distorted and eikonal wave functions, respectively, to approximately represent the distortion effects of the Coulomb potentials in both the entry and exit channels,

$$\begin{aligned}\chi_{\rm i}^{(+)\rm CDW} &= \Phi_{\rm i}^{\rm B}(\mathrm{R_P},\mathrm{r_T})F^{(+)}(a_{\rm P},-\mu\boldsymbol{v}_{\rm i},\boldsymbol{r}_{\rm P})\\ &\quad\times F^{(+)}(a_{\rm i},\boldsymbol{v}_{\rm i},\boldsymbol{R})\mu^{-{\rm i}a_{\rm P}}, \qquad (1)\\ \Psi_{\rm f}^{(-)\rm EFS} &= \Phi_{\rm f}^{\rm B}(\mathrm{R_T},\mathrm{r_P})E^{(-)}(a_{\rm T},\boldsymbol{v}_{\rm f},\boldsymbol{r}_{\rm T})E^{(-)}(a_{\rm f},\boldsymbol{v}_{\rm f},\boldsymbol{R}), \qquad (2)\end{aligned}$$

where $\boldsymbol{v}_{\rm i,f}$ are the incoming positron and outgoing Ps velocities and $\Phi_{\rm i,f}^{\rm B}$ are the unperturbed initial and final states. $F^{(+)}$ and $E^{(-)}$ are the continuum distorted and eikonal phase factors, respectively. μ is the reduced mass of the positron to electron. ($\boldsymbol{r}_{\rm T}$, $\boldsymbol{R}_{\rm P}$), ($\boldsymbol{r}_{\rm P}$, $\boldsymbol{R}_{\rm T}$) and ($\boldsymbol{R}$, $\boldsymbol{r}$) are three pairs of Jacobi coordinates for the present three-body systems (see, for example, Ref [22]). In the continuum distorted wave function of Eq. (1), the long-range Coulomb interactions of the target atoms or ions and the incident positron can be naturally taken into account at all asymptotic domains of coordinate space and momentum space.[23,24]

Once the wave functions in both channels are determined, the use of either post or prior form makes no differences in calculation. Here we use the prior form to construct the transition matrix. The distortion potential $W_{\rm i}$ for the initial wave function $\chi_{\rm i}^{\rm CDW}$ can be derived from the system Hamiltonian analytically,

$$\begin{aligned}(H-E)\chi_{\rm i}^{\rm CDW} &= W_{\rm i}\chi_{\rm i}^{\rm CDW}\\ &= \left(\frac{1}{M_{\rm P}}\nabla_{\boldsymbol{r}_{\rm P}}\cdot\nabla_{\boldsymbol{R}}-\frac{1}{M_{\rm T}}\nabla_{\boldsymbol{r}_{\rm T}}\cdot\nabla_{\boldsymbol{R}}\right.\\ &\quad\left.-\frac{1}{m}\nabla_{\boldsymbol{r}_{\rm T}}\cdot\nabla_{\boldsymbol{r}_{\rm P}}\right)\chi_{\rm i}^{\rm CDW}, \qquad (3)\end{aligned}$$

where $M_{\rm P}$, m, and $M_{\rm T}$ are the positron, electron and nucleus mass, respectively. The perturbation $W_{\rm i}$ can be considered as the difference between the exact initial-state interaction among all three particles and the approximate scattering potential used to calculate $\chi_{\rm i}^{\rm CDW}$.

The prior form of the exact transition matrix element is given by the two-potential formula[25]

$$\begin{aligned}T_{\rm fi}^{\rm EFS-CDW} &= \langle\Psi_{\rm f}^{(-)\rm EFS}|W_{\rm i}|\chi_{\rm i}^{(+)\rm CDW}\rangle\\ &\quad+\langle\Phi_{\rm f}^{\rm B}|V_{\rm f}^{\dagger}-W_{\rm i}|\chi_{\rm i}^{(+)\rm CDW}\rangle, \qquad (4)\end{aligned}$$

where the channel interaction for final state $\Phi_{\rm f}^{\rm B}$ is

$$V_{\rm f}=\frac{1}{R}-\frac{1}{r_{\rm T}}. \qquad (5)$$

The following steps to calculate the differential and integrated cross sections are straightforward.

The EFS-CDW method has close relationship with the Born approximation due to the fact that it includes the entire first- and second- and partial three- and higher-orders of Born expansion series. It is useful to rewrite the transition matrix element Eq. (4) to

$$\begin{aligned}T_{\rm fi}^{\rm EFS-CDW} &= \langle\Phi_{\rm f}^{\rm B}|V_{\rm f}^{\dagger}|\chi_{\rm i}^{(+)\rm CDW}\rangle\\ &\quad+\langle\Psi_{\rm f}^{(-)\rm EFS}-\Phi_{\rm f}^{\rm B}|W_{\rm i}|\chi_{\rm i}^{(+)\rm CDW}\rangle. \qquad (6)\end{aligned}$$

The first amplitude corresponds to the B-CDW model introduced by Bransden *et al.*[26] and the second term contains all remaining corrections due to the final state. Reminding the multiple scattering theory of Dewangan and Khadkikar,[27] it can be derived that the first term can be constructed as[28]

$$\langle\Phi_{\rm f}^{\rm B}|V_{\rm f}^{\dagger}|\chi_{\rm i}^{(+)\rm CDW}\rangle = T_{(1)}^{\rm B}+T_{(2)}^{\rm B}+T_{(3)}^{\rm B(a)}+\widetilde{T}_{(3)}^{\rm B(b)}+\cdots \qquad (7)$$

where

$$\begin{aligned}T_{(1)}^{\rm B} &= \langle\Phi_{\rm f}^{\rm B}|V_{\rm f}^{\dagger}|\Phi_{\rm i}^{\rm B}\rangle = \langle\Phi_{\rm f}^{\rm B}|(V_{\rm eT}+V_{\rm pT})^{\dagger}|\Phi_{\rm i}^{\rm B}\rangle, \qquad (8)\\ T_{(2)}^{\rm B} &= \langle\Phi_{\rm f}^{\rm B}|V_{\rm f}^{\dagger}G_0^{(+)}V_{\rm i}|\Phi_{\rm i}^{\rm B}\rangle\\ &= \langle\Phi_{\rm f}^{\rm B}|(V_{\rm eT}+V_{\rm pT})^{\dagger}G_0^{(+)}(V_{\rm pe}+V_{\rm pT})|\Phi_{\rm i}^{\rm B}\rangle, \qquad (9)\\ T_{(3)}^{\rm B(a)} &= \langle\Phi_{\rm f}^{\rm B}|V_{\rm f}^{\dagger}(G_0^{(+)}V_{\rm pe}G_0^{(+)}V_{\rm pe}\\ &\quad+G_0^{(+)}V_{\rm pT}G_0^{(+)}V_{\rm pT})|\Phi_{\rm i}^{\rm B}\rangle, \qquad (10)\\ \widetilde{T}_{(3)}^{\rm B(b)} &= \langle\Phi_{\rm f}^{\rm B}|V_{\rm f}^{\dagger}|[\Phi_{\rm i}^{\rm B}]^{-1}[G_0^{(+)}V_{\rm pe}\Phi_{\rm i}^{\rm B}][G_0^{(+)}V_{\rm pT}\Phi_{\rm i}^{\rm B}]\rangle. \qquad (11)\end{aligned}$$

The Coulomb potentials V_{pT}, V_{pe}, and V_{eT} describe the positron–nucleus, positron–electron, and electron–nucleus interactions and $G_0^{(+)}$ is the free Green's function of the system satisfying the outgoing boundary condition. It is therefore concluded that various multiple-scattering processes, especially the Thomas double-scattering,[29,30] appear naturally in the present model.

3. Results and discussions

3.1. Differential cross sections

The differential cross sections provide more details of the scattering mechanism than the integrated ones in investigating the Ps formation process. In Fig. 1, differential Ps(1s–4s) formation cross sections for H(2s) by positron impact at 50 eV are displayed separately and compared with the DWT calculations of Ghoshal and Mandal[13] where they are available. It is clearly seen that the present results are in good agreement with those obtained by DWT at both small and large angles except that, at intermediate angles about 30°–60°, the DWT results show a deep minimum around 40° (the DWT result for Ps(4s) formation at 40° is zero in Ref. [13] and it cannot be shown in log scale) while the present EFS-CDW model has a more complicated structure. In our calculations a multi-dimensional integration in computing the transition matrix (Eq. (4)) is the only step performed numerically (all remaining are analytical, for details see Ref. [18]), we have increased the integration points from 2×10^7 to 5×10^7 for all scattering angles to avoid any numerical errors. These two calculations are indistinguishable in the present scale, as we can see from Fig. 1, which implies the oscillation structure is an intrinsic character under the present approximation.

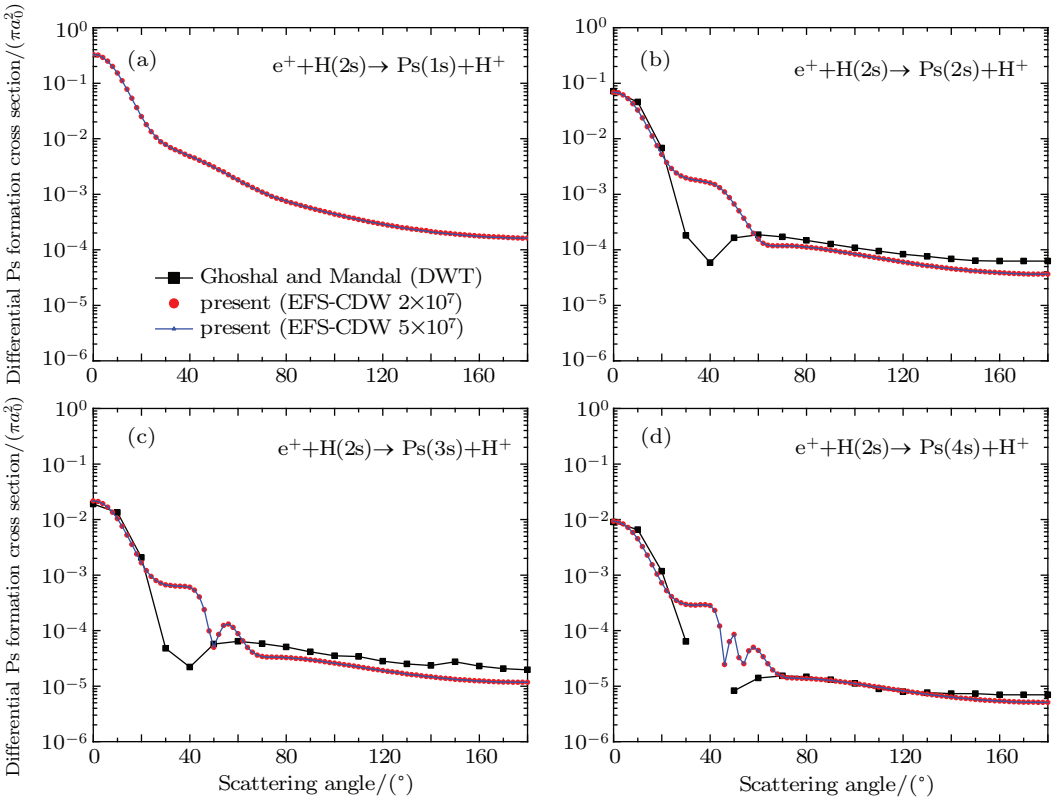


Fig. 1. (color online) Differential (a) Ps(1s), (b) Ps(2s), (c) Ps(3s), and (d) Ps(4s) formation cross sections for positron impact on H(2s) at 50 eV. The results of DWT method by Ghoshal and Mandal[13] are shown for comparison.

It is well known that the minimum in DWT method is formed due to the destructive interference of the higher angular momentum states of the scattered waves, if a partial-wave expansion of the transition matrix is performed.[13] Such structure exists extensively in all kinds of distorted wave methods as well as the first-order Born approximation. In the present EFS-CDW model, the complicated structure at about 45° corresponds entirely on the multiple-scattering mechanism including the Thomas double-scattering, which is a natural result of the second- and higher-orders of Born expansion series. The relationship between the present EFS-CDW method and the Born expansions has been discussed above. Details of the scattering mechanism of Thomas double-scattering in either quantum or classical pictures are available everywhere[19,29,30] and will not be discussed here. Another quite interesting phenomenon is the increasing of oscillation characters of the Thomas peak when Ps is formed in higher s-states. It should be attributed to the radial distributions of the Ps atom in different s-states where multi-shell structures exist. Very similar structures as those in Fig. 1 are also obtained for the differen-

tial cross sections of Ps(1s–4s) formation for positron impact on H in ground state (results are not shown here).

It should be mentioned here that although our results differ significantly from the calculations of DWT at intermediate angles, the integrated cross sections are generally the same due to the forward character of the Ps formation process. The differential cross sections are highly peaked at 0° and fall rapidly at large angles. Although the calculation of Ps differential cross sections makes no further difficulties in various theoretical methods, there are enormous difficulties in experimental measurements of such quantity. It is just recently available that the first absolute differential Ps formation cross sections are measured for several noble gas atoms and small molecules.[31] It is highly expected that the differential Ps formation cross sections for H might be available in the near future.

3.2. Integrated cross sections

The integrated cross sections are readily obtained by integrating the differential cross sections. In Fig. 2, we display the Ps(1s–4s) formation cross sections from each thresholds to 1000 eV. Both FBA and DWT results of Ghoshal and Mandal[13] are included for comparison. Similar DWT calculations were performed by Nayek and Ghoshal,[14,15] however, mostly for plasma screening environment. Here we only include their results in pure Coulomb situation. The pioneering calculation of Fojón *et al.*[11,12] for Ps(1s) formation was also included in Fig. 2. The CBA results generally follow the same trend as the prediction of DWT and FBA in high energy region while they are much closer to our EFS-CDW calculations at relatively low energies. It is surprisingly found that the CBA results continuously increase as the incident energy approaches to the threshold (see also Fig. 2 of Ref. [12]). Reminding the fact that, for many targets in either ground or metastable states such as the alkali-metal atoms[32,33] and He atom in 1s2s(^{3}S) state,[17] their Ps formation thresholds are all negative and their cross sections would always decrease when the positron incident energy approaches to zero. In our present calculation of Ps(1s) formation, the cross sections start to decrease at about 10 eV. For all Ps(1s–4s) formations, our results agree reasonably well with the predictions of DWT except that, for energies larger than 100 eV, ours are generally smaller in magnitude. In such relatively high energy range, the DWT method reduces to FBA method due to the Born transition term dominates the scattering amplitudes. For the present EFS-CDW method, the continuum distorted factor in the initial scattering wave function contributes small at higher energies, while the Eikonal phase factor in the exit channel still has significant suppression on the Ps formation cross sections. This can be seen in Ref. [21] where the B-CDW method follows the same trend as the FBA method in high energy range. However, it is known that the inclusion of Eikonal phase factor in exit channel is responsible to produce the correct behavior at low energies. Such factor may overestimate the distortion effect in high energy scattering.

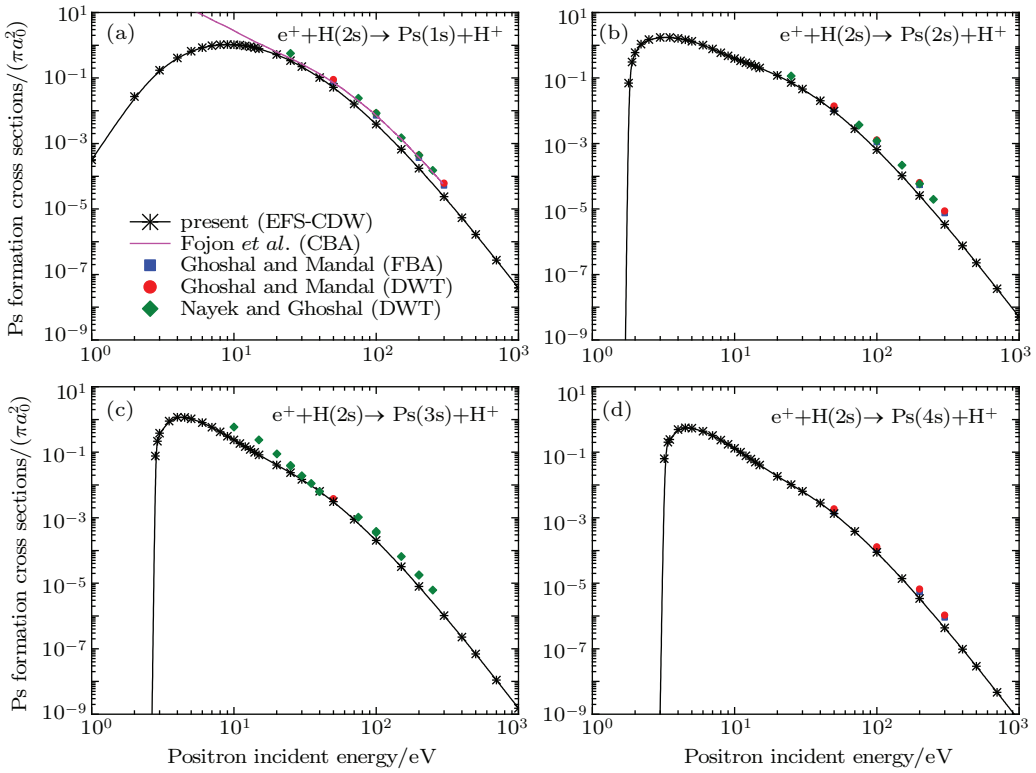


Fig. 2. (color online) Integrated (a) Ps(1s), (b) Ps(2s), (c) Ps(3s), and (d) Ps(4s) formation cross sections for positron impact on H(2s). The results of CBA model by Fojó *et al.*,[11,12] FBA and DWT methods by Ghoshal and Mandal[13] and Nayek and Ghoshal[14,15] are shown for comparison.

We show in Fig. 3 the Ps(2p–5p) formation cross sections where there are no other calculations available in the literature. The Ps(np) formation cross sections exhibit almost the same pattern as the Ps(ns) ones. For energies between 10 eV–20 eV, there exist low-lying flat structures in both the Ps(np) and Ps(ns) ($n \geq 2$) cross sections. Possible reasons will be discussed later. It has been several years that Charlton[34] has proposed a wave vector matching model which implies a fact that the Ps formation cross sections are largest when the positron incident energy is in the vicinity of twice the relevant threshold energy. It is based on the simple hypothesis that Ps forms most likely when the wave vectors of the incoming positron and the outgoing Ps atom are matched. Our recent work shows that such criterion works very well for various positronium formation process of H and H-like ions in their ground states. The present Ps(2s) and Ps(2p) formation cross sections both locate a maximum at about 3.5 eV, which is almost twice of the corresponding threshold (1.7 eV).

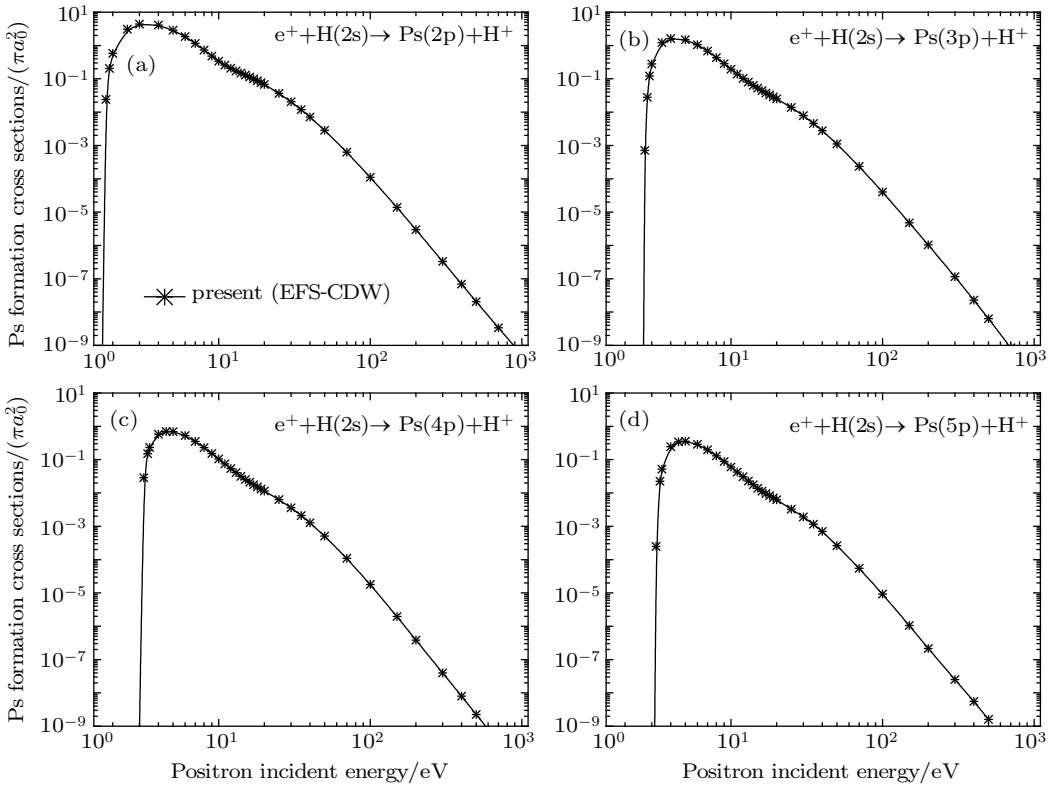


Fig. 3. Same as Fig. 2 but for Ps(2p–5p) formations.

Making summations over all s- and p-state Ps formations, the Ps(n) formation cross sections are obtained approximately and they are displayed in Fig. 4. The Ps(3d, 4d, and 4f) are relatively small in our calculations and they are negligible in the summations. Also shown in Fig. 4 are those for H in ground state by the present method which are in good agreement with other state-of-art calculations and experiment results (for details, see Ref. [18]). It is surprisingly found that, at relatively low impact energies, Ps formation occurs mostly when the electron is captured into $n = 2$ shell. At relatively high energies, our calculation shows that the Ps(n) formation cross sections follow the n^{-3} scaling law very well, as those for H(1s). From Fig. 4 it is also clear that the low-lying flat structures mentioned above at 10 eV–20 eV is due to the competition effects of Ps formation in different final states. At about 10 eV, Ps(1s) formation achieves its maximum and the possibilities of Ps formation into other states would be somewhat fewer. The distinct behavior for Ps(n) formation cross sections for position scattering with H(1s) and H(2s) states are related to the channel opening thresholds. For positron-H(1s) scattering, all Ps formation channels are opening at positive energies. The maximum positions predicted by present and other theoretical methods (see Ref. [18]) are almost twice the thresholds which can be well explained by the wave-vector matching model.[34] The maximum positions shift to higher energies for higher Ps(n) states. For positron-H(2s) scattering, the Ps(1s) channel threshold energy is negative, while higher Ps(n) thresholds are larger than zero. At present there is no such empirical law for predicting the maximum position of Ps formation for atoms with negative threshold energy. For Ps(n = 2, 3, and 4) formations where the channel opening thresholds are positive, their maximum positions are almost twice the corresponding threshold energies which are in good agreement with the wave-vector matching model.

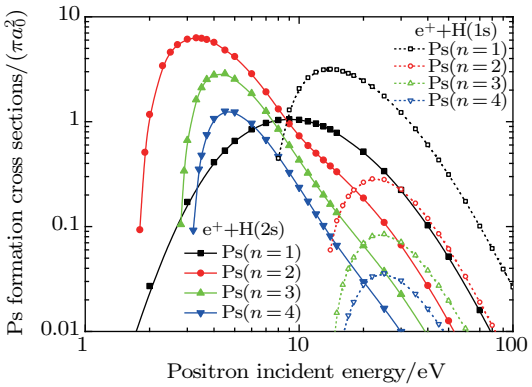


Fig. 4. (color online) Ps(n = 1–4) formation cross sections. Full lines with solid symbols and dash lines with hollow symbols are for positron impact on H(2s) and H(1s), respectively.

3.3. Total cross sections

We sum all the Ps(n = 1–4) formation cross sections as the total Ps formation cross sections because those for Ps(n) ($n \geq 5$) are expected to be very small due to the n^{-3} scaling law. The total cross sections for positron impact on H in the ground state by the present method are also shown in Fig. 5 for comparison with the ability of the present method to reproduce the experimental results and other state-of-art theoretical calculations demonstrated in the inset. Both the results of CBA by Fojón *et al.*[11,12] and DWA by Ghoshal *et al.*[13–15] are for Ps formations in s-state only and, furthermore, at relatively high energies. Their results are not proper to be compared with in the present figure scale. However, for the DWT method, a clue can be drawn from the inset that their predictions for H(1s) target overestimate the Ps formation cross sections at low impact energies.

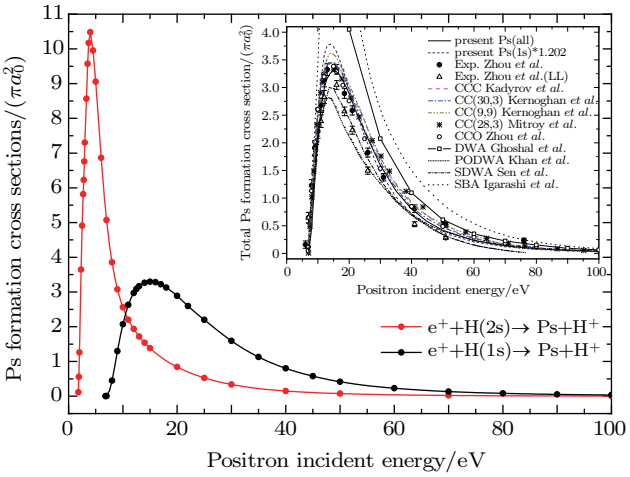


Fig. 5. (color online) Total Ps formation cross sections for positron impact on H(2s) and H(1s). Also shown in the inset are the comparison of the Ps formation cross sections of H(1s) with other theoretical calculations and experimental measurements. For details of the references, see Fig. 7 of Ref. [18].

From Fig. 5, it is generally concluded that the total Ps formation cross sections for positron scattering from H(2s) state are significantly larger at low energies, while smaller at intermediate and high energies, compared with those from hydrogen in ground state. The maximum position is located at about 4 eV due to the largest contribution is attributed to the Ps formation into $n = 2$ shell. The largest value of the cross section is almost 3 times larger than that for H(1s). An interesting comparison has also been made by Utamuratov *et al.*[17] for the Ps formation by positron impact on metastable helium in $1s2s^3S$ state, where the cross sections are also much larger than those for He target in ground state and its maximum position is also shifted to extremely low energies.

4. Conclusions

In this work, we have applied the EFS-CDW model to investigate the differential, integrated, and total Ps formation cross sections for positron scattering from metastable H in 2s state. Our results are compared with other theoretical calculations available in the literature such as CBA, FBA and DWT methods. The calculated differential cross sections agree well with the DWT predictions, however, with a multi-scattering structure appearing at about 45° which is an intrinsic feature of the present model. The integrated cross sections for Ps(1s) formation generally have a similar trend as other calculations at relatively high energies except that, at low energies, our results decrease rapidly while CBA increase continuously when the positron energy approaches to the threshold. More calculations are warranted to shed light on this energy range. In our calculations, Ps(n = 2) formations dominate the total Ps formation cross sections for energies below 10 eV and, in higher-energy ranges, the n^{-3} scaling law is well kept. Comparison with the Ps formation process for H in ground state shows that the total Ps formation cross sections for positron scattering from H(2s) state are significantly larger at relatively low energies, while smaller at high energies. We expect our work could provide useful informations for further studies.

References

[1] Charlton M 1985 *Rep. Prog. Phys.* **48** 737
[2] Charlton M and Humberston J W 2001 *Positron Physics* (Cambridge: Cambridge University Press)
[3] Surko C M, Gribakin G F and Buckman S J 2005 *J. Phys. B: At. Mol. Opt. Phys.* **38** R57
[4] Nagashima Y 2014 *Phys. Rep.* **545** 95
[5] Laricchia G, Armitage S, Kövér A and Murtagh D J 2008 *Adv. At. Mol. Opt. Phys.* **56** 1
[6] Chiari L and Zecca A 2014 *Eur. Phys. J. D* **68** 297
[7] Ma J, Cheng Y, Wang Y C and Zhou Y 2011 *J. Phys. B: At. Mol. Opt. Phys.* **44** 175203
[8] Bohr A, Blickle A, Paolini S, Ohlinger L and Forrey R C 2012 *Phys. Rev. A* **85** 042710
[9] Tantawi R S and Nagah A 2015 *Can. J. Phys.* **93** 1360
[10] Nassar T E I and Tantawi R S 2015 *Phys. Scr.* **90** 015402
[11] Fojón O A, Gayet R, Hanssen J and Rivarola R D 1995 *Phys. Scr.* **51** 204
[12] Fojón O A, Gayet R, Hanssen J and Rivarola R D 1995 *Phys. Scr.* **52** 607

[13] Ghoshal A and Mandal P 2008 *J. Phys. B: At. Mol. Opt. Phys.* **41** 175203
[14] Nayek S and Ghoshal A 2012 *Phys. Plasmas* **19** 113501
[15] Nayek S and Ghoshal A 2013 *Phys. Scr.* **88** 045301
[16] Hanssen J, Hervieux P A, Fojón O A and Rivarola R D 2000 *Phys. Rev. A* **63** 012705
[17] Utamuratov R, Kadyrov A S, Fursa D V, Bray I and Stelbovics A T 2010 *Phys. Rev. A* **82** 042705
[18] Jiao L, Wang Y and Zhou Y 2011 *Phys. Rev. A* **84** 052711
[19] Jiao L, Wang Y and Zhou Y 2012 *J. Phys. B: At. Mol. Opt. Phys.* **45** 085204
[20] Zhang Y Z, Yu R M, Li S X, Song X D and Jiao L G 2015 *J. Phys. B: At. Mol. Opt. Phys.* **48** 175206
[21] Macri P A, Miraglia J E, Hanssen J, Fojón O A and Rivarola R D 2004 *J. Phys. B: At. Mol. Opt. Phys.* **37** L111
[22] Macri P A 2006 *Nucl. Instrum. Methods B* **247** 75
[23] Kim Y E and Zubarev A L 1997 *Phys. Rev. A* **56** 521
[24] Jones S and Madison D H 2002 *Phys. Rev. A* **65** 052727
[25] Gell-Mann M and Goldbergerv M L 1953 *Phys. Rev.* **91** 398
[26] Bransden B H, Joachain C J and McCann J F 1992 *J. Phys. B: At. Mol. Opt. Phys.* **25** 4965
[27] Dewangan D P and Khadkikar S B 1985 *J. Phys. B: At. Mol. Opt. Phys.* **18** L751
[28] Chen X Y, Wen B, Xu Y W and Zheng Y Y 1992 *J. Phys. B: At. Mol. Opt. Phys.* **25** 4661
[29] Toshima N and Eichler J 1991 *Phys. Rev. Lett.* **66** 1050
[30] Igarashi A, Toshima N and Ishihara T 1992 *Phys. Rev. A* **46** 5525
[31] Shipman M, Armitage S, Beale J, Brawley S J, Fayer S E, Garner A J, Leslie D E, Van Reeth P and Laricchia G 2015 *Phys. Rev. Lett.* **115** 033401
[32] Le Anh-Thu, Bromley M W J and Lin C D 2005 *Phys. Rev. A* **71** 032713
[33] Lugovskoy A V, Kadyrov A S, Bray I and Stelbovics A T 2010 *Phys. Rev. A* **82** 062708
[34] Charlton M 2006 *J. Phys. B: At. Mol. Opt. Phys.* **39** 4575